

# A New Approach to Detect Hypernuclei and Isotopes in the QMD Phase Space Distribution at Relativistic Energies

A. Le Fèvre<sup>1</sup>, J. Aichelin<sup>2</sup>, Ch. Hartnack<sup>2</sup>, Y. Leifels<sup>1</sup>  
(<sup>1</sup>GSI Darmstadt, Germany; <sup>2</sup>Subatech Nantes, France)

## Abstract

We developed an improved clusterisation algorithm which aims at predicting more realistically the yields of clusters in the framework of the Quantum Molecular Dynamics model. This new approach is able to predict isotope yields as well hypernucleus production at relativistic energies. To illustrate its predicting power, we confront this new method to experimental data from 100 A.MeV to 2 A.GeV, with a closed view on isotope yields and flows, and show the sensitivity on the parameters which govern the cluster formation.

## Introduction

In heavy ion reactions at energies between 20 A.MeV and several GeV, many clusters are formed. This cluster formation presents a big challenge for transport models in which nucleons are the degrees of freedom which are propagated. In many approaches, the fragment formation is simply omitted, which invalidates the single particle observables as well, because the cluster formation depends on the phase space region and, therefore, single particle spectra are modified. Identifying clusters in a transport code which transports nucleons is all but simple. Quantum effects as well as range and strength of the different parts of the nuclear potential, like bulk, symmetry energy and pairing, in a complicated environment at finite temperature, influence the fragment yield.

## Simulated Annealing Clusterisation Algorithm: The principles

If we want to identify fragments early, while the reaction is still going on, one has to use the momentum as well as the coordinate space informations. The idea how to do this has been introduced by Dorso et al. [1] and it has been further developed into the Simulated Annealing Clusterisation Algorithm (SACA) [2]. This approach consists in the following steps: starting from the positions and momenta of the nucleons at a given time, nucleons are combined in all possible ways into fragments or single nucleons. Neglecting the interaction among nucleons in different clusters, but taking into account the interaction among the nucleons in the same fragment, this algorithm identifies that combination of fragments and free nucleons which has the highest binding energy. It has been shown that clusters obtained by that approach are the pre-fragments for the final state clusters. The reason for this is the fact that fragments are not a random collection of nucleons at the end, but an initial-final state correlation. The advantage of the SACA approach, as compared to other methods which rely only on proximity in coordinate space, like MST (“Minimum Spanning Tree”) [3], is the possibility to identify fragments quite early during the heavy ion reaction. This has been demonstrated in [4], in which is also shown that MST gives only reliable results after 200-400 fm/c whereas SACA identifies the fragment already shortly after the high density phase of the heavy ion collision. This is crucial, because the fragment partitions can reflect the early dynamical conditions (Coulomb, density, flow details, strangeness...).

## Improving the prediction of isotope production

Our goal is to improve the description of the fragment yields within the scope of the QMD transport code. In its initial version, SACA contains as ingredients only the potentials which are responsible for the average binding energy of the clusters: a volume component (Skyrme mean field) which dominates, and a correction for surface effects in the form of a Yukawa potential. This version has already shown its strong predictive power concerning the fragment yields within the scope of the BQMD transport model [9, 10].

If we want to extend our model to predict the absolute multiplicity of the isotope yields, we have to add new features to the SACA cluster identification like asymmetry energy, pairing and quantum effects. For the asymmetry energy, we use the parametrisation from IQMD [5] which we use in the present article as transport code for the transport of nucleons:

$$E_{asy} = E_0 \left( \frac{\langle \rho_B \rangle}{\rho_0} \right)^{\gamma-1} \frac{\rho_n - \rho_p}{\rho_B}$$

where  $E_0=32$  MeV,  $\gamma=1$  (“stiff” asymmetry potential), and  $\rho_n$ ,  $\rho_p$ ,  $\rho_B$ ,  $\rho_0$  are, respectively, the neutron, proton, baryonic and saturation densities.

Another significant part of the binding energy of light isotopes are the shell and odd-even effects (pairing). In the conditions of high pressure and temperature where SACA is used to determine the pre-fragments, these structure effects are not well known. E. Khan et al. in [6] showed that there are some indications that they affect the primary fragments. The authors demonstrate that the pairing vanishes above a nuclear temperature  $T_V \approx 0.5\Delta_{pairing}$  (pairing energy). At normal density the pairing energy tends to be negligible for heavy nuclei, with  $\Delta_{pairing} = \frac{12}{\sqrt{A}} MeV$ , whereas it is strong for light isotopes, like  ${}^4He$  and  ${}^3He$  with 12 MeV and 6.9 MeV, respectively. In SACA the primary fragments are usually produced quite cold, with  $T < 1 - 2 MeV$ , and hence below  $T_V$ . The description of Khan et al. applies to the saturation density,  $\rho_0$ , but pairing effects have to vanish at high or low density which SACA clusters may reach. Therefore we use the computed pairing densities for each isotope which is created by SACA and apply a correction factor of the  $\rho_0$  pairing energy, depending on the cluster density. In [7], within the Hartree-Fock-Bogoliubov method, Khan et al. have derived the following function for the pairing potential

$$V_{pairing} = V_0 \left( 1 - \eta \frac{\rho(r)}{\rho_0} \right) \delta(\mathbf{r}_1 - \mathbf{r}_2)$$

where  $\eta$  provides the surface-to-volume character of the interaction ( $\eta=1$  or  $0$  would mean pure surface or volume interaction, respectively). We have adopted this parametrisation to derive a correction factor  $f_\eta(\langle \rho_B \rangle)$  depending on the mean density of the fragment which is applied to the deviation

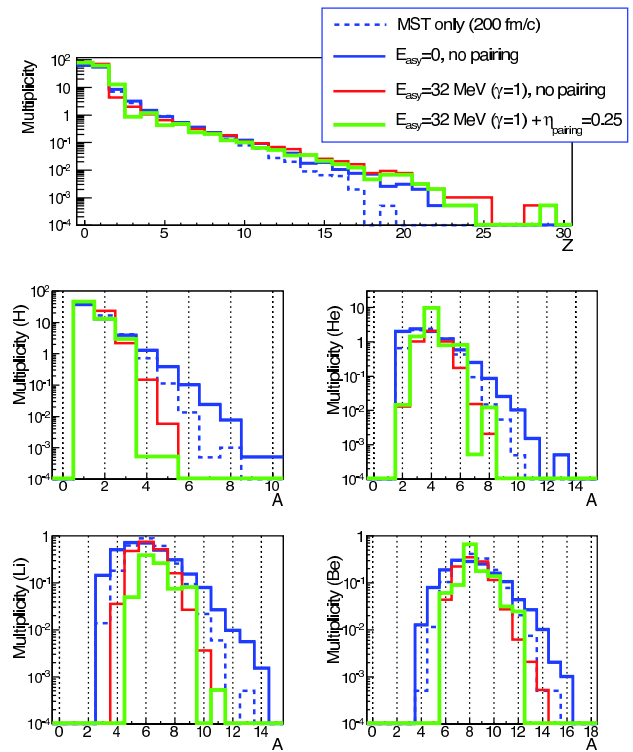


Figure 1: IQMD predictions for the central ( $b < 0.2b_{max}$ ) collisions of  ${}^{124}Xe + {}^{112}Sn$  at 100 A.MeV incident energy. Dashed line for the MST (coalescence) algorithm alone (performed at the late time 200 fm/c), blue line for the initial SACA model, which has been implemented an asymmetry term (red) and additional pairing contribution (green). The top panel shows the mean multiplicity distribution of fragments as a function of their charge. The four others depict the yields of H, He, Be and Li isotopes.

of the binding energy with respect to the Bethe-Weizsäcker formula (liquid drop model) without pairing term  $\Delta B_{pairing}(N, Z, \rho_0)$ . The “structure” contribution to the binding energy of a nucleus (N,Z) at baryonic density  $\rho_B$  would then become  $\Delta B_{pairing}(N, Z, \rho_B) = \Delta B_{pairing}(N, Z, \rho_0) f_\eta(< \rho_B >)$ . Isotopes which are not stable at all in nature, are discarded in SACA by assigning to them a very repulsive  $\Delta B_{pairing}$ . Fig. 1 shows the influence of the asymmetry energy and of the pairing energy of the isotope yield in the reaction  $^{124}\text{Xe} + ^{112}\text{Sn}$  at 100 A.MeV which has been measured by the INDRA ref.[8]. We display here the results for central collisions ( $b < 0.2b_{max}$ ). We have obtained the best agreement with the INDRA data of ref.[8] for the light isotope yields using  $\eta = 0.25$ . This figure illustrates as well how the various ingredients influence the fragments yield obtained in SACA, assuming an early clusterisation at  $t=60$  fm/c where pre-fragments are already stabilised in size. We see that the charge distributions are not strongly modified by the ingredients, whereas details of the isotopic yield are strongly influenced: the asymmetry energy tends to narrow the distributions towards the valley of stability, and the pairing component tends to restore the natural abundances.

## How the dynamical patterns of isotopes are affected

The way the fragments are formed has an important side effect on the dynamical features, as shown in fig. 2. There, we see that the ratios of the transversal and of the longitudinal width of the momentum distributions for those isotopes whose binding energy is strongly modified (tritons,  $^3\text{He}$ ,  $^4\text{He}$ ) is strongly influenced by the new ingredients of SACA, which do not affect at all neutrons and protons. Any study of the flow of light fragments should take care of that aspect.

## Excitation energy and density of the primary fragments

The pre-fragments, called also “primary” fragments, created in SACA, are often produced non relaxed in shape and density. Going back to their ground state shape and density creates an excitation energy, whose dependence on the fragments size and on the incident energy of the projectile is depicted in fig. 3. Here, the excitation energy is calculated as the difference between the binding energy of the fragment obtained by SACA and the experimentally measured value, and we include in SACA the asymmetry and “pairing” contributions. We note that at low bombarding energy (100 A.MeV), for  $Z > 1$ , where a large fraction of the fragments is formed from participant matter, the primary fragments have on the average 2 A.MeV excitation energy. This value is close to the 3 A.MeV of S. Hudan et al. in [11] that have been derived experimentally for central Xe+Sn at the somehow lower (50 A.MeV) incident energy. This excitation energy is sufficiently large to cause a significant contribution of the secondary decay of the pre-fragments to the yield of small clusters. On the contrary, at relativistic energies, heavier fragments are produced from spectator matter and are therefore much colder on the average. The contribution from secondary decay is getting negligible, except for He and Li. Another interesting feature of the primary clusters in SACA is their internal density. Fig. 4 shows its dependence on the fragments size and on the incident energy. Although the medium is close to  $\rho_0$  at this early stage of the collisions (60 and 40 fm/c for 100 and 600 A.MeV bombarding energy, respectively), the clusters are produced very dilute, around  $\rho = \rho_0/6$ . This is explained by the fact that the dense clusters are disfavoured, because they would contain nucleons which are flowing against each other. In this case the nucleons have a too high relative momenta to form a cluster. Therefore only the low density behaviour of the potentials, which are contributing to the binding energy, is important for the fragment formation.

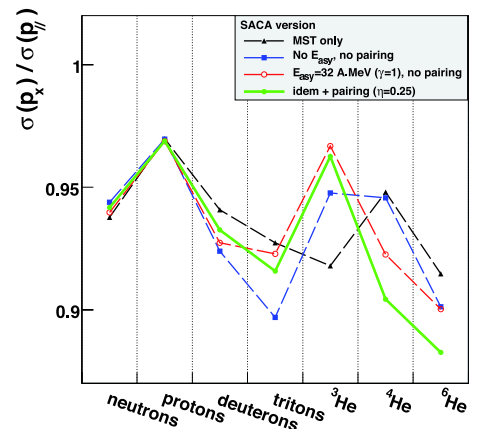


Figure 2: The ratio of the width of the transversal and of the longitudinal momentum distribution (with respect to the reaction plane) for various light isotopes for the same parametrisations of the potential as used in fig. 1.

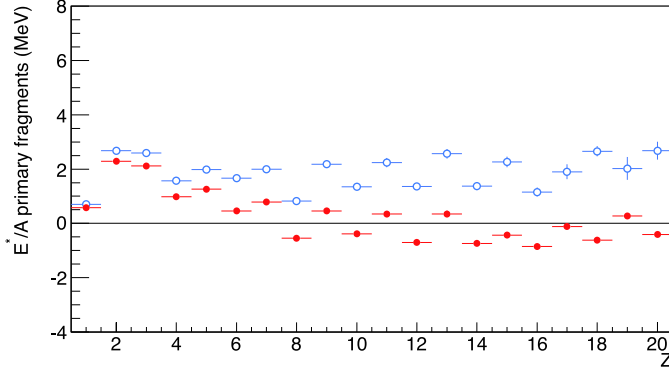


Figure 3: Mean excitation energy of fragments as a function of their charge as predicted by IQMD+SACA (with all binding energy ingredients) for central ( $b < 0.2b_{max}$ ) collisions of  $^{124}\text{Xe} + ^{112}\text{Sn}$  at 100 A.MeV (open blue symbols) and  $^{197}\text{Au} + ^{197}\text{Au}$  at 600 A.MeV (full red symbols) incident energy.

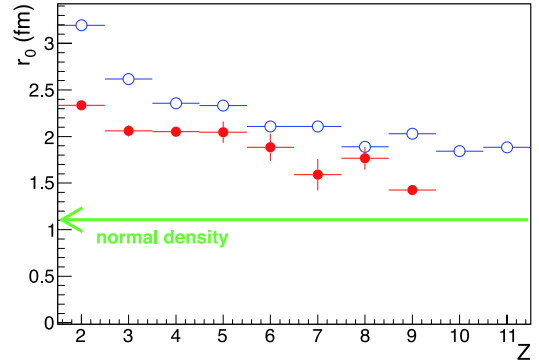


Figure 4: The same as fig. 3 for the mean radius of primary fragments.

## About the apparent vanishing of the asymmetry term in pre-fragments at high energy

Are the contributions of the asymmetry and pairing energy for the fragment formation energy dependent? This question has been raised by the FOPI Collaboration in [12]. There, the mean  $^3\text{He}$  and  $^4\text{He}$  multiplicities in central collisions of Au+Au are shown as a function of the beam energy, see Fig. 5. Whereas at low energy (around 100 A.MeV), the  $^4\text{He}$  dominates the  $^3\text{He}$  production by an order of magnitude, above the A.GeV, the contrary is the case. For IQMD-SACA, one obtains a very good agreement with the experimental data at low energy only if asymmetry and pairing energies are included. The domination of  $^3\text{He}$  at higher energies, on the contrary, is not reproduced yet: only if one switches off in SACA the asymmetry and pairing terms, the high energy data can be reproduced. We are presently investigating the origin for this observation. .

## Another application of SACA : hypernuclei production

A hypernucleus is a nucleus which contains at least one hyperon ( $\Lambda(uds)$ , ...) in addition to nucleons. Extending SACA to the strange sector requires the knowledge of the  $\Lambda N$  potentials. For a first study, we consider the strange quark as inert and use  $V_{\Lambda N} = \frac{2}{3}V_{nN}$  for protons as well as for neutrons. Using this potential, SACA produces hypernuclei with the same algorithm as for non strange fragments. In the underlying IQMD program, which propagates the hadrons,  $\Lambda$ 's are produced in different reactions:  $K + N \rightarrow \Lambda + \pi$ ,  $\pi + n \rightarrow \Lambda + K^+$ ,  $\pi^- + p \rightarrow \Lambda + K_0$ ,  $p + p \rightarrow \Lambda + X$ . Their abundance, position and momentum distributions are strongly influenced by the reaction kinematics, the nuclear equation of state and the in-medium properties of the  $K^+$  (kaon potential, etc.) which are implemented in the transport model.

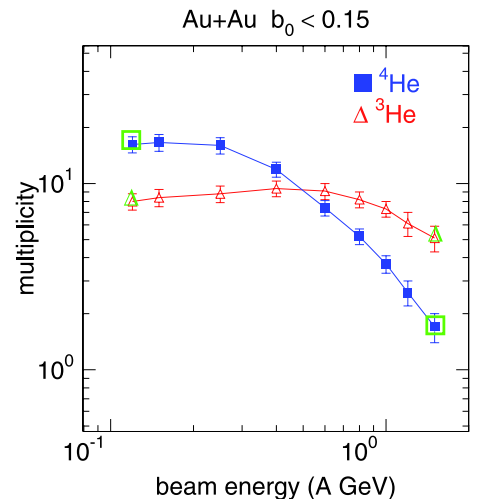


Figure 5:  $^3\text{He}$  (triangles) and  $^4\text{He}$  (squares) mean multiplicities as a function of the beam energy in central Au+Au collisions measured by FOPI (red and blue symbols) [12]. The green symbols correspond to the IQMD predictions, using SACA with (at low beam energy) or without (at high beam energy) asymmetry and pairing potentials in the pre-fragments formation.

To have a realistic description of the production of hypernuclei over the wide mass range which can be measured in relativistic heavy-ion collisions is a challenging task because it demands to reproduce correctly, within the present scope, all details which influence the creation of an hypernucleus. They can be subdivided into the three following steps : first, we have to know the yield, the positions and the momenta of the hyperons at the time of clusterisation, second, we have to know the hyperon-nucleon interaction potential which determines the probability that a hyper nucleus prefragment is formed and third we have to reproduce the properties of the hyperisotopes which are formed. Whereas the first step depends on the transport modelisation, the two others depend on the SACA parametrisation. As an illustration of this extension of SACA towards the hypernucleus production applied to IQMD simulations, fig. 6 shows the predicted yields of a wide variety of light hypernuclei in semi-central collisions of  $^{58}\text{Ni} + ^{58}\text{Ni}$  at 1.91 A.GeV bombarding energy, for a clusterisation time  $t = 20\text{fm}/c$ .

Fig. 7 shows the rapidity distributions of tritons,  $\Lambda$ 's and hypertritons ( $d + \Lambda \rightarrow_{\Lambda} t$ ), where we see that the hypertritons, though similar in mass and charge to the tritons, are produced in a very different phase space, mostly in the fireball - mid-rapidity region, like the  $\Lambda$ 's, whereas the tritons are mainly following the spectator regions. In comparison with the  $\Lambda$ 's, we observe that the hypertriton rapidity distribution is flatter, extending more towards the spectators, because this is where the yields of the deuterons are peaked, which are needed to create them.

## Conclusions

We present here the first step towards an understanding of the production of isotopic yields and hypernuclei in heavy ion reactions. The production of these particles has up to now been beyond the scope of transport models. Improving SACA by including pairing and asymmetry energies and hence by a more precise description of the nucleus, allows for realistic predictions of absolute isotope yields, and of hypernuclei. We have seen that the asymmetry and pairing potentials can have a strong influence on the momentum anisotropies (i.e. apparent stopping power) for the isotopes (tritons,  $^3\text{He}$ ,  $^4\text{He}$ , ...). According to this model the nucleons which form fragments have initially a low density. They contract and form finally slightly excited fragments. Therefore fragment formation is sensitive to the density dependence of the asymmetry energy and the pairing energy. However, fragments test this dependence only for densities below saturation density.

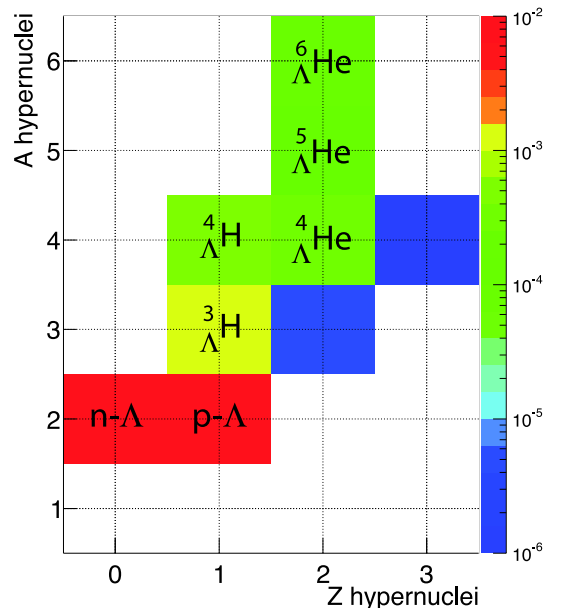


Figure 6: Yields of hypernuclei as predicted by IQMD+SACA for semi-central collisions (corresponding to the most central half of the total cross-section) of  $^{58}\text{Ni} + ^{58}\text{Ni}$  at 1.91 A.GeV incident energy. Here, SACA contains no asymmetry and pairing terms. The clusterisation is done at  $t=20\text{fm}/c$ , and IQMD uses a soft equation of state, a momentum dependant interaction and a kaon potential of 20 MeV.

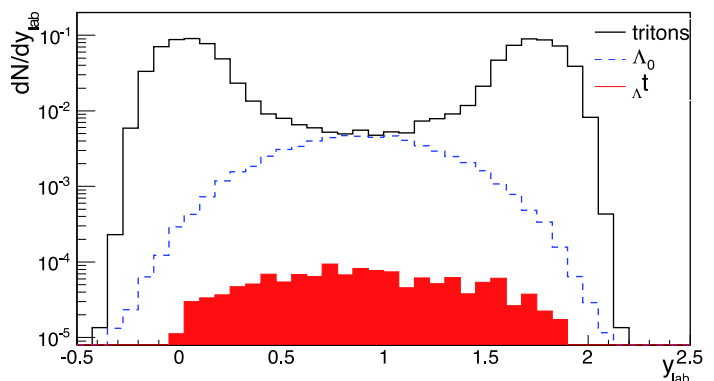


Figure 7: For the same system as in fig. 6, the predicted rapidity distributions of tritons (full black line),  $\Lambda$ 's (dashed blue line) and hypertritons (red filled area).

For the dependence on densities higher than normal nuclear matter density, one has to focus on “elementary” particles which are produced in the most dense phases of the collisions, like  $\Delta$ s, kaons or pions. Still unclear is why SACA fails to describe the  ${}^3\text{He}$  and  ${}^4\text{He}$  yields at high beam energies when including pairing and asymmetry potentials.

Further developments in SACA are needed and on the way. We have to employ more realistic  $\Lambda\text{N}$  potentials, secondary decays have to be taken into account at low beam energies and the treatment of fragments with a short lifetime has to be improved.

## References

- [1] C. O. Dorso and J. Randrup, Phys. Lett. B **301**, 328 (1993).
- [2] R. K. Puri and J. Aichelin, J. Comput. Phys. **162**, 245 (2000).
- [3] J. Aichelin, et.al., Phys. Rev. **202** (1991).
- [4] P.B. Gossiaux, R. Puri, Ch. Hartnack, J. Aichelin, Nucl. Phys. A **619** (1997) 379-390.
- [5] Ch. Hartnack et al., Eur. Phys. J. A **1** (1998) 151.
- [6] E. Khan, Nguyen Van Giai, N. Sandulescu, Nucl. Phys. A **789** (2007) 94.
- [7] E. Khan, M. Grasso and J. Margueron, Phys. Rev. C **80** (2009) 044328.
- [8] A. Le Fèvre et al., Nucl. Phys. A **735** (2004) 219-247.
- [9] K. Zbiri, A. Le Fèvre, J. Aichelin et al., Phys. Rev. C **75** (2007) 034612.
- [10] A. Le Fèvre et al., Phys. Rev. C **80** (2009) 044615.
- [11] S. Hudan et al. (INDRA collaboration), Phys. Rev. C **67** (2003) 064613.
- [12] W. Reisdorf and the FOPI Collaboration, Nucl. Phys. A **848** (2010) 366-427.